SLAS Technology 29 (2024) 100118

Contents lists available at ScienceDirect

SLAS Technology

journal homepage: www.elsevier.com/locate/slast

Full Length Article

ANDeS: An automated nanoliter droplet selection and collection device

Joaquín E. Urrutia Gómez [a], Razan El Khaled El Faraj [a], Moritz Braun [c], Pavel A. Levkin [a,b,*], Anna A. Popova [a,*]

[a] Institute of Biological and Chemical Systems – Functional Molecular Systems (IBCS-FMS), Karlsruhe Institute of Technology, Hermann-von-Helmholtz Pl. 1, Eggenstein-Leopoldshafen 76344, Germany
[b] Institute of Organic Chemistry, Karlsruhe Institute of Technology, Kaiserstraße 12, Karlsruhe 76131, Germany
[c] Institute for Applied Materials - Ceramic Materials and Technologies, Karlsruhe Institute of Technology (KIT), Haid-und-Neu straße 7, Karlsruhe 76131, Germany

ARTICLE INFO

Keywords:
Droplet microarray
Miniaturization
High throughput
Liquid handling
Automation

ABSTRACT

The Droplet Microarray (DMA) has emerged as a tool for high-throughput biological and chemical applications by enabling miniaturization and parallelization of experimental processes. Due to its ability to hold hundreds of nanoliter droplets, the DMA enables simple screening and analysis of samples such as cells and biomolecules. However, handling of nanoliter volumes poses a challenge, as manual recovery of nanoliter volumes is not feasible, and traditional laboratory equipment is not suited to work with such low volumes, and small array formats. To tackle this challenge, we developed the **A**utomated **N**anoliter **D**rop**l**et **S**election device (ANDeS), a robotic system for automated collection and transfer of nanoliter samples from DMA.

ANDeS can automatically collect volumes from 50 to 350 nL from the flat surface of DMA with a movement accuracy of ±30 μm using fused silica capillaries. The system can automatically collect and transfer the droplets from DMA chip into other platforms, such as microtiter plates, conical tubes or another DMA. In addition, to ensure high throughput and multiple droplet collection, the uptake of multiple droplets within a single capillary, separated by air gaps to avoid mixing of the samples within the capillary, was optimized and demonstrated.

This study shows the potential of ANDeS in laboratory applications by using it for the collection and transfer of biological samples, contained in nanoliter droplets, for subsequent analysis. The experimental results demonstrate the ability of ANDeS to increase the versatility of the DMA platform by allowing for automated retrieval of nanoliter samples from DMA, which was not possible manually on the level of individual droplets. Therefore, it widens the variety of analytical techniques that can be used for the analysis of content of individual droplets and experiments performed using DMA. Thus, ANDeS opens up opportunities to expand the development of miniaturized assays in such fields as cell screening, omics analysis and combinatorial chemistry.

1. Introduction

Miniaturized high throughput platforms have become essential tools for research and development over the last 35 years [1,2]. Such technologies enable assay volumes to be reduced down to nanoliters, equivalent to a volume a thousand times smaller than the volumes used in conventional platforms. Moreover, they increase the number and variety of samples, allowing a broader range of experimental conditions to be explored in a single experiment [3,4]. As a result, these platforms effectively minimize chemical and sample consumption, reducing operational costs [5]

The Droplet Microarray (DMA) (Fig. 1A) is a platform that enables miniaturization and parallelization of diverse assays. It consists of a coated microscope glass slide, where the surface is chemically functionalized to create a hydrophilic-superhydrophobic array pattern [6]. This pattern facilitates the formation of an array of hundreds nanodroplets. This method allows for the manufacture of DMAs with different droplet sizes, geometries and densities. Unlike traditional platforms, DMA does not require wells or reservoirs to hold the liquid. Instead, each droplet is precisely positioned and immobilized on the planar surface of the slide. Hydrophilic-superhydrophobic pattern enables not only confinement of nanoliter volumes, which is not possible in microtiter plates with physical barriers between the well, but also through its planarity compatibility with dispensing and retrieval of the droplets [7].

* Corresponding authors at: Institute of Biological and Chemical Systems – Functional Molecular Systems (IBCS-FMS), Karlsruhe Institute of Technology, Hermann-von-Helmholtz Pl. 1, Eggenstein-Leopoldshafen 76344, Germany.
E-mail addresses: pavel.levkin@kit.edu (P.A. Levkin), anna.popova@kit.edu (A.A. Popova).

https://doi.org/10.1016/j.slast.2023.11.002
Received 18 August 2023; Received in revised form 4 October 2023; Accepted 14 November 2023
Available online 18 November 2023

The easy access to the hydrophilic spots of DMA permits the addition of hundreds to thousands of droplets in a precise, fast and homogeneous manner by using commercially available low volume non-contact liquid dispensers [8–10]. However, retrieval of nanoliter droplets from the DMA is important and remains challenging due to the small volume and size of the droplets.

The DMA platform is compatible with various analytical techniques, including optical microscopy, [11,12]. IR/Raman spectroscopy, desorption electrospray ionization mass spectrometry (MS), [13] matrix-assisted laser desorption ionization (MALDI) [14]. Such compatibility has allowed the miniaturization of chemical and biological assays, for instance the development of high-throughput screening of cancer drugs in patient-derived cells [15] or the establishment of high-throughput screening of functional hydrogels libraries [16]. However, there are currently challenges in interfacing certain analytical devices with the DMA. Some examples of these devices are liquid chromatography-mass spectrometry (LC-MS), nuclear magnetic resonance (NMR), real-time PCR systems, and gel electrophoresis equipment. The incompatibility between these instruments and the DMA is mainly due to the lack of commercially available instrumentation suitable for handling droplet-based microarrays. Although some liquid handling devices offer a degree of versatility, they fall short in performing tasks associated with droplet workflows. These tasks include droplet generation, merging, transferring, addressing, positioning, capturing and sorting [17]. Moreover, most droplet-based microarrays are tailored to specific applications, which makes their integration with commercially available equipment even more challenging. As a result, there has been an increased inclination towards the development of customized platforms and in-house techniques aimed at improving adaptability. Notable examples of automated platforms include SODA (Sequential Operation Droplet Array), designed for precise manipulation and analysis of picoliter-scale droplets, [18] and DropLab, an automated microfluidic platform for programming nanoliter droplet-based reactions [19]. Furthermore, innovative solutions have emerged to address the challenge of integrability into analytical workflows. Among these solutions are methods employing capillaries to directly transport nanoliter droplets into analytical systems, such as high-speed capillary electrophoresis, [20] as well as unique solutions such as a swan-shaped probe for direct interfacing into an electrospray ionization mass spectrometer (ESI-MS) [21].

The challenge to overcome the compatibility of DMA with a wider range of analytical instruments lies in the development of a method to collect and transfer nano-droplets. Three criteria arise in this regard:

(i) Handling small volumes: The small volumes involved make manual handling impractical or even impossible. For instance, with droplets as small as 200 nL, precision becomes crucial, given their height of 350 μm on a 1 mm^2 hydrophilic base. In addition, the close proximity between droplets, down to 500 μm, further complicates the process, making the use of automation a necessity.

(ii) Dead volume: Whereas losses on the order of nanoliters due to sample handling may be considered negligible in larger assays, they become substantial when working at the nanoliter scale. Therefore, it is essential to minimize dead volume to ensure reliable sample analyses.

(iii) Control of evaporation: When working with nanodroplets that are exposed to the environment, rapid evaporation becomes a significant concern. To mitigate this problem, sample collection methods must be exceptionally fast or implemented in a manner that effectively prevents evaporation.

Solving these challenges is the key to expanding the potential of DMA, as it would open doors to a wider range of analytical read-out methods and equipment. A remarkable example that meets these three criteria is the work of Councill et al. [22,23] in which a commercial pipetting robot was successfully reconfigured to handle individual collection of nanoliter droplets. This approach enabled the study of low-input proteomic samples contained in droplets by liquid chromatography-mass spectrometry.

To address the challenge of droplet retrieval on DMA, we developed the **A**utomated **N**anoliter **D**rop**l**et **S**election and collection device (**ANDeS**) (Fig. 2), an automated system designed to assist in the collection and transfer of nanoliter droplets from the DMA to other

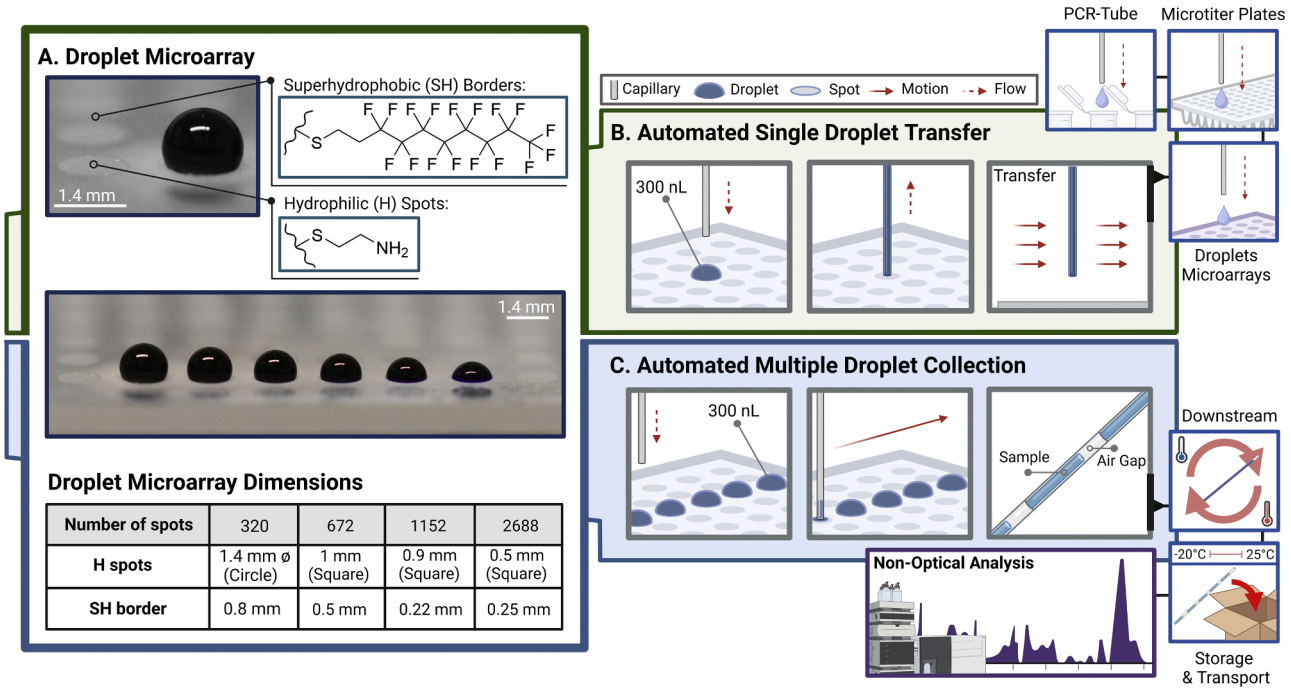

Fig. 1. The concept of automated nanodroplet collection from Droplet Microarray (DMA). (A) A photo of a DMA slide showing droplets ranging from 2 μL to 500 nL. The accompanying table presents the dimensions of hydrophilic (H) spots, superhydrophobic (SH) borders, and the corresponding number of droplets per a 2.5 × 7.5 cm DMA slide. (B) Schematic workflow for single-drop transfer from a DMA to other platforms. (C) Schematic workflow for multiple droplet collection from a DMA, conducting *in-capillary* processing, storage of samples, and final analysis using non-optical analysis platforms.

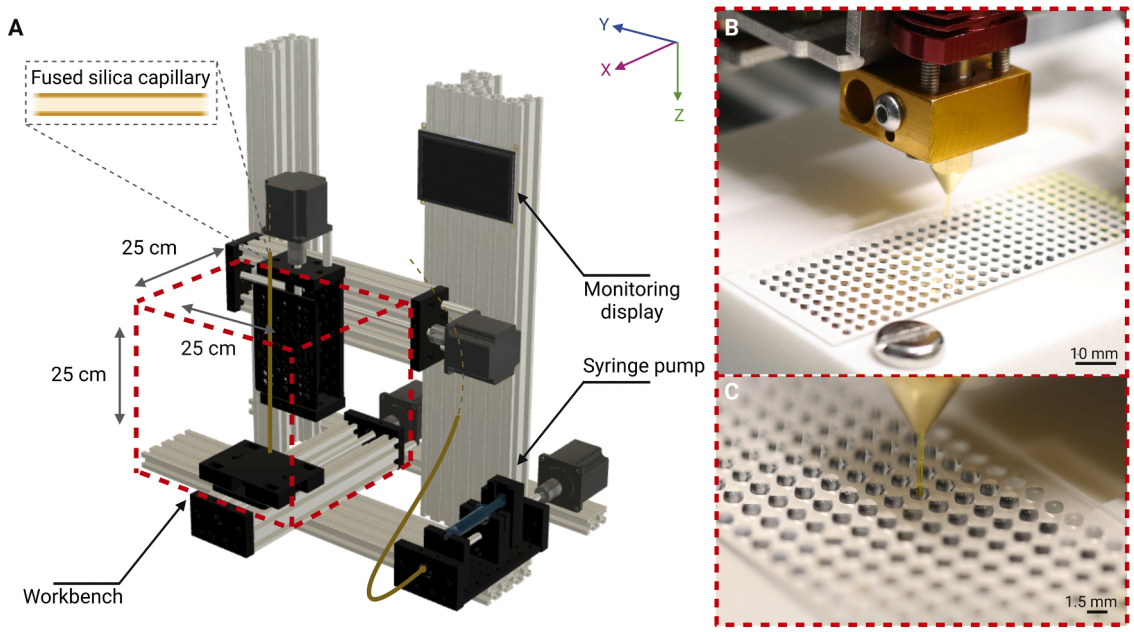

Fig. 2. Depiction of the main characteristics of the ANDeS (A) 3D renderings of the ANDeS based on a CAD model. The dashed box represents the work station. (B, C) The workbench images display the capillary holder nozzle with a diameter of 360 μm Ø, as well as a DMA consisting of 320 spots with a round shape of 1.4 mm diameter. Each spot contains 1 μL of water droplets.

platforms for further analysis. The ANDeS combines a 3-axis motion system with a syringe pump (Fig. 2A). By utilizing the syringe pump, the device enables the collection of droplets through a fused silica capillary, which serves a dual-purpose: nozzle and sample container. The sequential collection of multiple droplets within a single capillary offers flexibility in adjusting the quantity and sorting of samples to be collected. This approach also facilitates the storage, transport, and transfer of samples to other platforms or measurement equipment (Fig. 1B and C). The ANDeS system offers a precise and reproducible collection of volumes ranging from 50 nL to 350 nL. Its mechanical components ensure a positional accuracy of ±30 μm, allowing the capillary tip to be positioned down to a DMA-spot area of 500 μm^2.

The findings of this study highlight the potential of ANDeS to enhance the versatility of the Droplet Microarray, making it compatible with analytical devices that were previously incompatible with its format. This approach opens up opportunities for the development of miniaturized assays in diverse areas, including cell and drug screening, omics, and combinatorial chemistry.

2. Results

In our study, we present ANDeS, an automated system designed, built, and validated for manipulating nanoliter droplets on a droplet microarray. ANDeS offers positional accuracy, adaptability to different droplet microarray formats and multi-drop collection. To asses ANDeS' effectiveness in supporting a routine laboratory procedure conducted using the DMA, we utilized it to collect multiple 350 nL samples and subsequently transfer them to analytical equipment. The results demonstrated that utilizing ANDeS not only enhanced procedural efficiency and eliminated human error but also improved result quality, surpassing manual sample collection methods.

2.1. Design and construction of the automated nanoliter droplet selection and collection device (ANDeS)

ANDeS is a 3-axis Cartesian plane motion system consisting of linear rails, carriages and transmissions. This system includes an integrated syringe pump, a high-resolution camera to record the process, and a touch-screen interface (Fig. 2A). The syringe pump is connected to a fused silica capillary (75 μm inner diameter, 360 μm outer diameter) via fittings. The capillary, acting as a replaceable nozzle, attaches to a Z-axis on a 3D printer hot-end extruder head to collect and relocate droplets (Fig. 2B). The movement of the leadscrews on each axis and the syringe pump is driven by Nema 17 bipolar stepper motors. The rotation of these motors are synchronized by A4988 stepper controllers, which receive steps and direction signals from a Raspberry Pi 4 through the Reprap Arduino Mega Pololu Shield 1.4 (RAMPS 1.4). The extra components such as the Raspberry Pi camera V2 and the touch screen display for controlling and monitoring, are connected directly to the microcontroller.

The positioning commands to place the capillary at the desired location within the work station are determined using an open-access graphical user interface (GUI), designed for a 3-axis robotic positioning system [21]. This GUI operates on an open-loop control algorithm, wherein stepper motors are directed according to a predefined sequence of movements and timing, devoid of real-time input from encoders or sensors to validate motor positions. The code computes the required step count for reaching the target position based on the distance to the target and a predefined step-to-distance ratio. As an example, for the 672 spots DMA, the array employed is 48 by 14 spots whit a distance between spots centers of 1.5 mm, this translates to a motor displacement of 37.5 steps between adjacent spots. Importantly, the upper-right spot serves as the designated home position. Within this GUI, the user can input different array lengths and spots distances, corresponding to different DMA formats. These inputs are automatically translated into motion parameters by the code. Additionally, we have incorporated control over the motor driving the syringe pump, allowing users to define the parameters to regulate the volume to be collected. The volume collected with ANDeS depends on three parameters: the volume of the syringe, the flow rate controlled by the syringe pump and the duration of the liquid uptake. The flow rate of the pump can be adjusted by modifying the revolutions per minute (RPM) and the number of motor steps through the GUI code, as described in Section 2.3. The duration of droplet uptake can be determined by the user in user interface while selecting the spots of interest. Different duration, and therefore collected volume, can be assigned to different spots within the

same run. Furthermore, the system allows for automatic loading of these instructions before each run to streamline the process.

2.2. Characterization of movement accuracy

To validate the precision of positioning of the capillary within the hydrophilic spots, we have used a DMA with square hydrophilic spots of 1000 μm side length and a distance between spot centers of 1500 μm, we calculated the positional accuracy of ANDeS as shown in Fig. 3 [24].

Accuracy refers to the ability of the axis to accurately reach a given position within the working area. For example, for the X-axis, this implies that it can be positioned with an error of up to ± 0.026 mm with respect to the intended target. On the other hand, positional uncertainty refers to the level of imprecision or variability in achieving those positions. Meaning that when the X-axis is commanded to move to a given location, it can deviate up to ± 0.143 mm from the intended position (Fig. 3). To obtain the values of accuracy and positional uncertainty in each axis, their translation from the reference point to the target position was measured in both directions, at a system maximum speed of 15 mm/second. This process was repeated 10 times. Once the data was obtained, the standard deviations of the distances obtained were calculated to determine the positional uncertainty of each axis. Then, the accuracy of each axis was estimated by calculating the Mean Squared Error (MSE). Finally, the MSE values of all axes were averaged to determine the overall accuracy, resulting in a combined MSE of ± 30 μm. This combined precision allows for precise control of the system, enabling accurate positioning of the capillary nozzle on arrays of various sizes, including microtiter plates and the DMA with 2688 spots (H spots: 0.5 mm (square); SH border: 0.25 mm) (Fig. 1A).

2.3. Characterization of droplet collection and transfer

In order to control the collection flow to pick up droplets of different sizes in only 1 second, we have first determined the dependencies of the collected volume and parameters like flow rate and motor frequency. To achieve this, we mounted a 100 μL syringe on the syringe pump and maintained a constant motor frequency of 3000 RPM. As a parameter of observation, we vary the number of steps executed by the motor during the collection of different experimental volumes. The measurements were carried out with water droplets using a capillary with a length of 150 cm and a diameter of 75 μm. The process was repeated three times for each of the six different volumes, ranging from 50 nL to 300 nL. Afterwards, the experimental data was used to develop an empirical model describing the relationship between collected volume, flow rate and motor steps (num_steps). The model followed a nonlinear regression equation $Flow = a\ exp\ (b\ num\_steps) + c$, as shown in Supplementary Fig. 1. When compared to experimental data, the model exhibited a coefficient of determination (R^2) of 0.9742, and a residual standard error (Sy.x) of 19.05. This indicates that the model can estimate the flow rate for collecting a single droplet of desired volume with an accuracy of ± 19 nL/s.

After establishing the droplet collection process, we validated the efficiency of ANDeS in transferring droplets from the DMA to other platforms, such as microtiter plates, vials and other DMAs. This validation aimed at applications related to the analysis of molecules collected or generated within the DMA. In such cases, the transfer of compounds from the DMA to other vessels becomes necessary for subsequent analysis by equipment such as for example PCR/qPCR machine, LC-MS or NMR. To evaluate the transfer process, we manually pipetted 300 nL of water onto a 1.4 mm Ø DMA spot, which was then automatically collected by ANDeS via capillary and transferred to another spot (Fig. 4A).

The height of the relocated droplet was measured and compared to its initial height before collection, as shown in Fig. 4C.

The volume of the droplets was calculated using the following equation for the volume of spherical cap: ($V = \sqrt{(4/3\pi)abc}$) (Fig. 4C), where a and b are the radius of the hydrophilic spot (according to the DMA of 1.4 mm Ø spots) and c is the height of the droplet. The calculated final volumes of the transferred droplets mean 308 nL with a 95 % confidence interval (CI) of ± 13 nL, corresponding to a measurement error of 1.2 %, $n = 10$. Accordingly, the results showed that an average volume of 2.9 % is lost when moving a drop from one point to another.

Once the volume loss associated with the droplet transfer process was determined, additional experiments were performed to show the capabilities of ANDeS to transfer droplets between different platforms. **Supplementary Video 1** illustrates the transfer of 250 nL droplets from a 1 mm square hydrophilic spot to a 1 μL droplet placed in a 1.4 mm Ø spot, with a transfer rate of ~ 30 s per droplet. In **Supplementary Video 2**, a 500 nL droplet is transferred from a 1.4 mm Ø DMA to a 250 μL conical tube. Then approximately 300 nL of water is withdrawn from another 250 μL conical tube and transferred back to the DMA. In this video, a speed of ~ 1 min per droplet is employed, representing the highest feasible operational speed to ensure sample integrity during

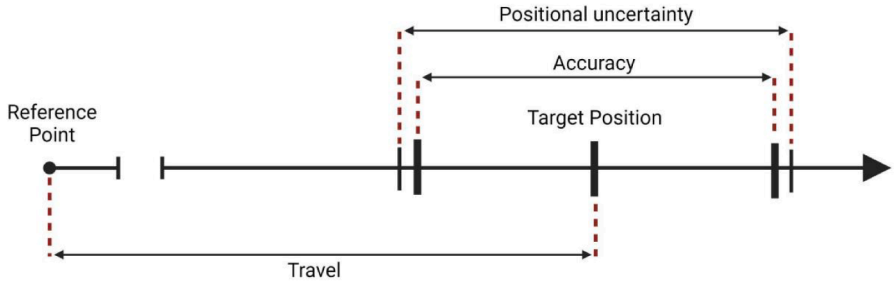

Axis	X (mm)	Y (mm)	Z (mm)
Travel	100	100	50
Accuracy	± 0.026	± 0.033	± 0.032
Positional uncertainty	± 0.143	± 0.156	± 0.127

Fig. 3. Characterization of positional accuracy of ANDeS. The schematic illustrates how the positional uncertainty and accuracy of ANDeS was estimated. To evaluate these parameters, each axis was moved in opposite directions over a given distance. The distance traveled by each axis was measured with a Mitutoyo 530–122 vernier caliper with a resolution of 0.02 mm. The table shows the values of travel, accuracy and positional uncertainty obtained for each axis ($n = 10$).

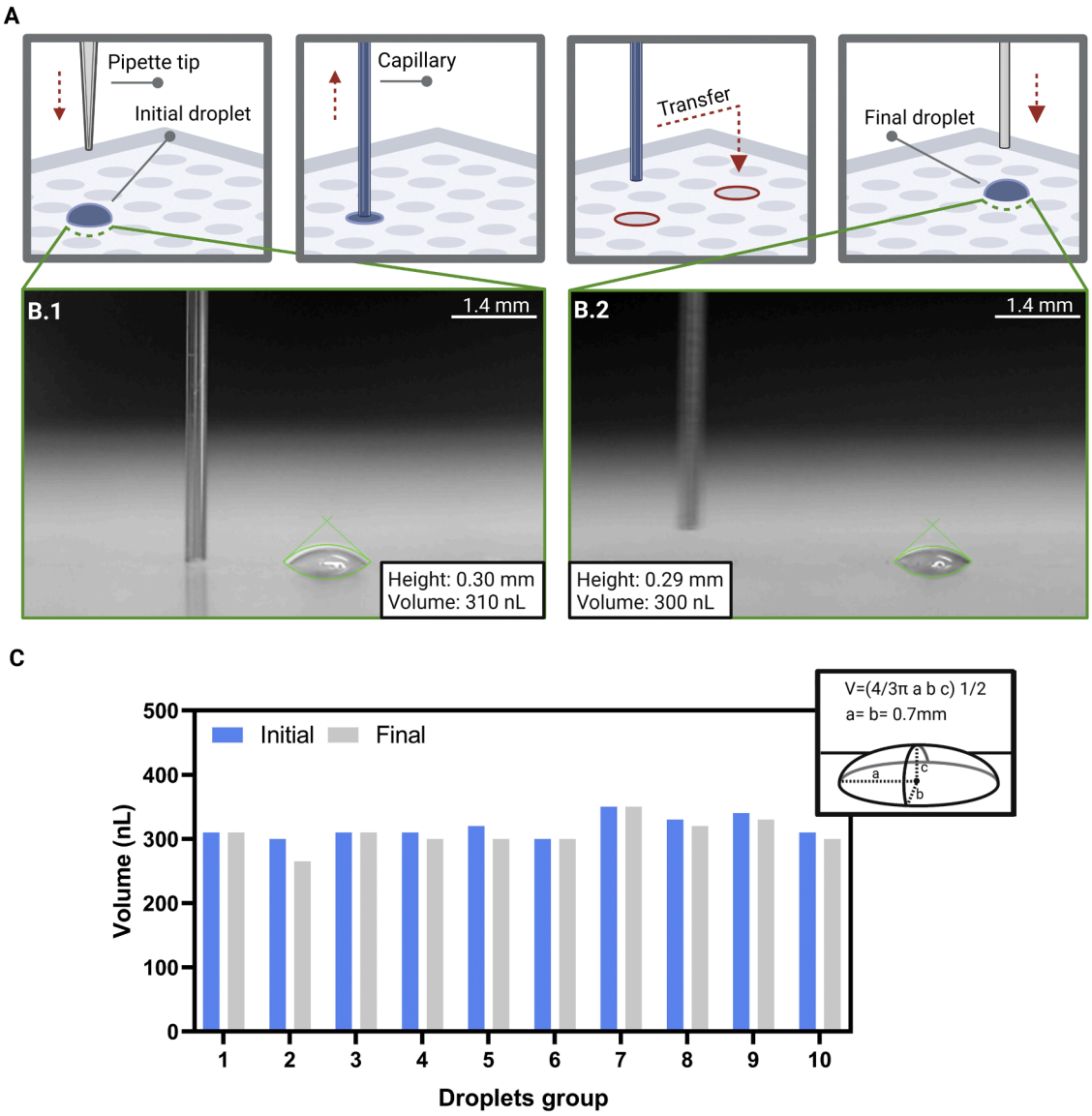

Fig. 4. Assessment of accuracy of droplet transfer. (A) Schematic representation of step-by-step automatic collection and relocation of a 300 nL droplet. (B.1) Analysis of droplet height and volume prior (B.2) and after the transfer. (C) Comparison of the volumes of droplets prior and after the transfer ($n = 10$).

transfer to platforms other than DMA. These videos showcase how ANDeS can assist in the automated collection of samples from the DMA and also provide sample transfer, especially when working with volumes that exceed the limitations of manual collection. The capacity to collect nanodroplets offers opportunities for sample analysis in the nanoliter range, eliminating the need to rely on volume ranges suitable for manual collection.

2.4. Characterization of multiple droplet collection

The utilization of fused silica capillaries for sample collection was chosen to meet specific requirements, such as the ability to accommodate multiple nanoliter samples, ease of handling, material durability, prevention of sample evaporation, and convenience in sample transport and storage. The capillaries also offer versatility in length and diameter, allowing them to contain different volumes and amounts of samples according to user preference. In addition, sample withdrawal from capillaries to other containers or platforms is a simple process that can be performed by ANDeS or manually using a syringe pump.

To validate the collection of multiple droplets, a DMA containing an array of 1 mm square hydrophilic spots was fully printed with 200 nL droplets using a non-contact liquid dispenser. Thereafter, six of these droplets were automatically collected by ANDeS using the same capillary. Finally, the lengths of the capillary the samples occupied (plugs) were determined using a light microscope, as depicted in Fig. 5A. To separate each sample from the previous one, an air plug of approximately 2.5 mm was created, which is determined by the time the capillary is suspended in the air without contact with the samples. The volume of the sample inside the capillary was calculated using the formula for cylindrical geometry ($V = \pi r^2 h$), where r is the internal radius of the capillary (37.5 μm) and h the length of the plug, which was measured between the center points of the meniscus at both ends of the sample (Fig. 5).

As shown in Fig. 5B, the volumes of collected droplets inside the capillary were calculated to be on mean 190 nL, with a 95 % CI of ± 2.6 nL, corresponding to a measurement error of 3 %, $n = 6$. Accordingly, these results showed that an average volume of 4.6 % is lost when collecting multiple droplets from the DMA.

For a total collection of 6 droplets, the time required was approximately 1 s per drop and 1 s waiting time between droplets to create the air plugs. Therefore, theoretically, employing an adequate syringe volume and adjusting the number of motor steps to match the syringe guage

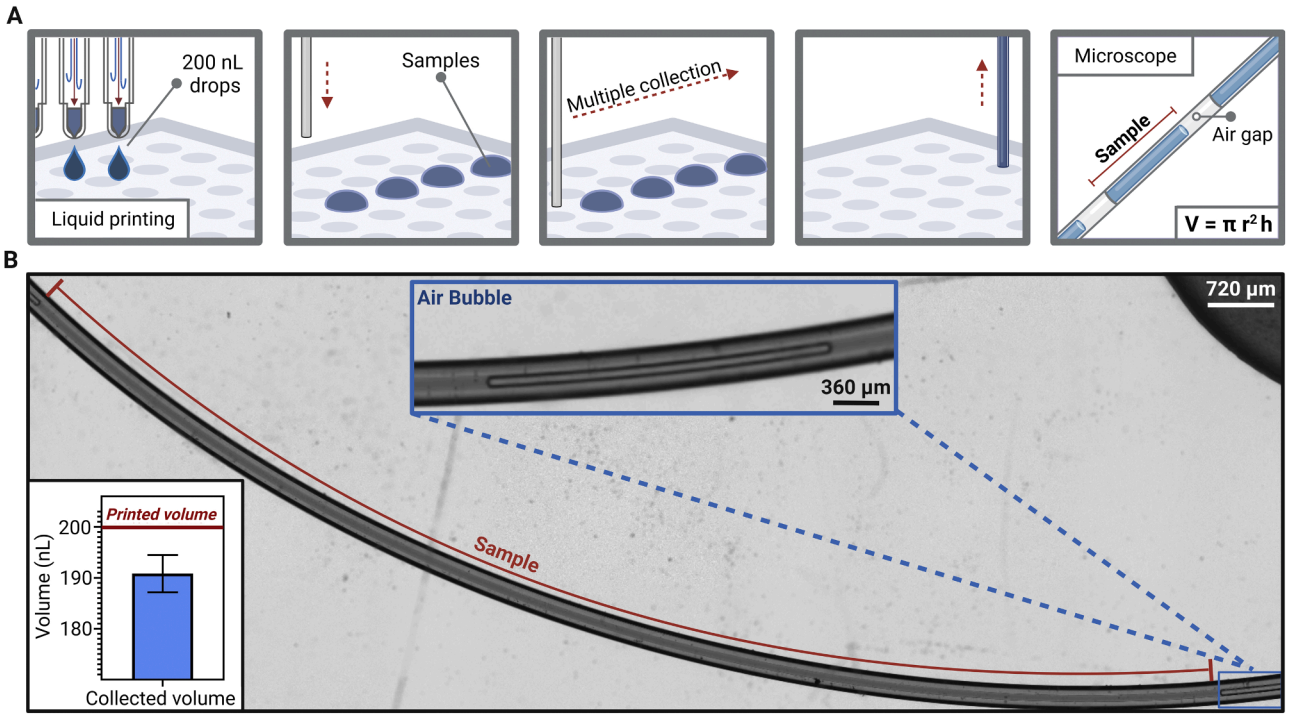

Fig. 5. Characterization of the automatic multi droplet collection. (A) Schematic workflow of the automatic multi droplet collection. (B) Image of a sample and an air plug between the samples inside fused silica capillary. In the lower left corner, the graph showing the measured volumes of the droplets collected inside the capillary compared to the initially printed volume of 200 nL. The red line represents the volume printed by the non-contact liquid dispenser. Error bar shows the standard deviation between 6 replicates each.

would make it possible to collect all 300 nL droplets from a 672-spot DMA in about 22 min when operating at the maximum frequency. An example of bulk collection can be seen in **Supplementary Video 3**, where 24 droplets of 300 nL were collected in 1 min and 20 s. This was performed at a rate of ~1.6 s per drop, which is the maximum collection rate to ensure a complete recovery of the droplets.

The possibility to collect several samples in a single capillary without mixing them, as shown in Section 2.5, offers the opportunity to perform in-capillary downstream processing. This can involve a number of techniques, such as thermal shocks, sonication or UV treatment. In addition, this format permits consecutive injection of these samples directly into analytical workflows, for example into a liquid chromatography system.

2.5. Demonstration of ANDeS for real-time experimental flow

In order to demonstrate the use of ANDeS for real lab application, we performed and validated the collection of cDNA samples from a DMA chip using the Cells-to-cDNA on Chip method [25]. In this method, the entire sample preparation process, including culturing and lysis of cells, isolation of mRNA and its conversion to cDNA, takes place in 200 nanoliter droplets. Although the protocol demonstrated high efficiency, the sample collection step had limitations. Since manual collection of individual nanoliter droplets is not feasible, the droplets were collected by pooling multiple droplets into a single conical PCR tube using larger volume of liquid. This method requires skilled users, does not allow for addressing individual droplets, and associated with a risk of sample loss and cross-contamination. To address this problem, we sought to validate automated collection of droplets containing cDNA and compared it to the manual procedure. For this, the samples of cDNA obtained in 350 nL droplets using the Cells-to-cDNA on chip protocol were collected manually and automatically (Fig. 6A and B). Each sample was then transferred to a single conical PCR tube for quantification of cDNA using qPCR analysis targeting the GAPDH (GlycerAldehyde 3-Phosphate DeHydrogenase) gene, as depicted in Fig. 6.

Obtained results demonstrate that the samples collected automatically using ANDeS exhibit average cycle threshold (CT) values for GAPDH gene, which reflect the concentration of cDNA in a sample, of 16.72 (Fig. 6C). This was comparable with GAPDH CT values of 16.88 in samples obtained through manual collection. Both samples collected automatically and manually had GAPDH CT values comparable to those in positive control (17.48), which was an original sample used for the test. Thus, these results demonstrate that the automated method for droplet collection is efficient and do not lead to the DNA loss during the transfer steps. Moreover, the automated method enables collection of each individual 672 droplets, which is not possible with manual droplet pooling. Pooling of multiple droplets as a method for their collection, requires labeling strategy in order to be able to distinguish the material from original droplets, ANDeS enables diverse samples to be collected and analyzed without the need for labeling prior to analysis. Additionally, the automated collection process preserves sample integrity by avoiding the need for sample dilution (during pooling process), reducing the risk of sample loss during the collection. It also minimizes human error and reduces collection time. For example, for an experienced laboratorian, collecting this group of 4 drops manually takes approximately 45 s, but with ANDeS, a group of 4 drops can be collected in only 8 s. On a larger scale, manual collection of 200 drops would require ~ 37 min, while the automated method would accomplish the task in only ~ 6 min.

As a next step, we validated the multiple droplet collection (MDC) method using the same cDNA sample approach. This method differs from the previous one, where droplets were collected individually and then pooled together in the same PCR tube. Instead, in the MDC, we collect all samples in the same capillary and analyze each droplet independently. As shown in Fig. 7, the MDC was used to collect 350 nL droplets of both cDNA and water within the same capillary. The addition of water droplets in this experiment permitted us to assess the potential for cross-contamination between collected samples when using the

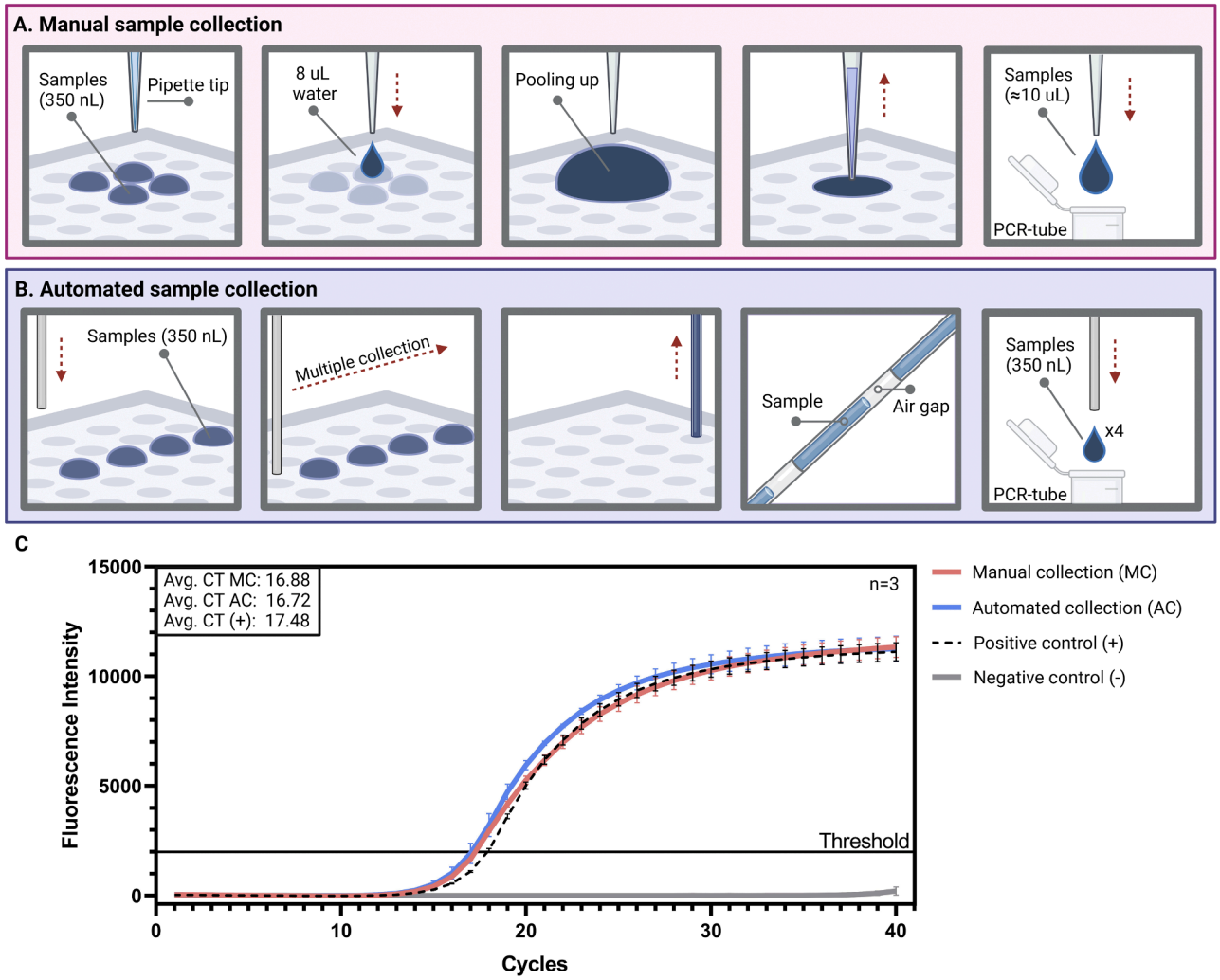

Fig. 6. Quality comparison of samples collected automatically and manually. (A) Schematic of the protocol for manual collection of nanoliter samples from a DMA. (B) Schematic of the protocol for automated collection of nanoliter samples from a DMA. (C) qPCR amplification curves of manual and automated collection of 22.6 ng/μl of cDNA synthesized by the Cells-to-cDNA on Chip method from SU-DHL-4 cells. (Avg. CT MC = Average Cycle Threshold Manual Collection; Avg. CT AC = Average Cycle Threshold Automatic Collection). Error bars show the standard deviation between 3 replicates each.

MDC. Once samples were collected, they were transferred to separate PCR tubes for subsequent qPCR analysis.

As shown in Fig. 7B, samples obtained from single 350 nL cDNA droplets exhibited a mean CT value of 19.42, indicating a successful amplification of the GAPDH target gene. The three water droplets introduced consecutively in the capillary showed mean CT values of 31.44, 37.26 and 39.16, respectively. According to the standards for qPCR diagnostic analysis, [26] CT values higher than 37 considered as a reasonable cut-off point to conclude the absence of the target gene in the sample. In order to assess cDNA contamination in the water droplets, we applied the conditional statement $x \leq Mean\ CTS \rightarrow x = 100; x \geq Cct \rightarrow x = 0$, where *Mean CTS* is the mean CT of the sample (19.42) and *Cct* is the cut-off value 37. Then, the percentage of cDNA contamination in these droplets was calculated as $Co = (Cct - x)/(Cct - Mean\ CTS)\ x\ 100$. Meaning that if the mean CT value of a water droplet is less than or equal to the *Mean CTS*, we considered the droplet 100 % contaminated. On the other hand, if the mean CT value of a water droplet is greater than or equal to the *Cct*, the water droplet is considered not contaminated. For droplets between these two thresholds, the percentage of contamination is calculated proportionally according to their position between the *Mean CTS* and the *Cct*. Using this method the following conclusions could be made: the first, closest to the cDNA sample, water drop exhibits a contamination percentage of Co = 31.7 %, the second drop shows Co = 7.4 % contamination, and the third drop demonstrates no apparent contamination with Co = 0 % (Fig. 7B). It is important to highlight that the qPCR technique has a very high sensitivity, capable of detecting DNA in samples at very low concentrations, even down to 10 pg/μL [27,28]. The results demonstrate a certain droplet-to-droplet contamination risk, which can be efficiently mitigated by adding two separate droplets of water between each sample droplet.

In this study, we utilized the quantitative polymerase chain reaction (qPCR) technique to effectively characterize the transfer and cross-contamination of multiple droplets collected within a single capillary. The findings highlight the performance of ANDeS in accurately collecting multiple nanoliter droplets. Moreover, our results underscore the potential of conducting qPCR analysis on nanoliter samples obtained from DMA. This research showcases the promising capabilities of ANDeS in enabling efficient nanoliter droplet collection and opens up new possibilities for high-precision droplet analyses.

3. Discussion

In this study, we developed and tested ANDeS, an automated device designed to overcome the challenge of retrieving nanoliter droplets from droplet microarrays (DMA) for subsequent transfer to analytical

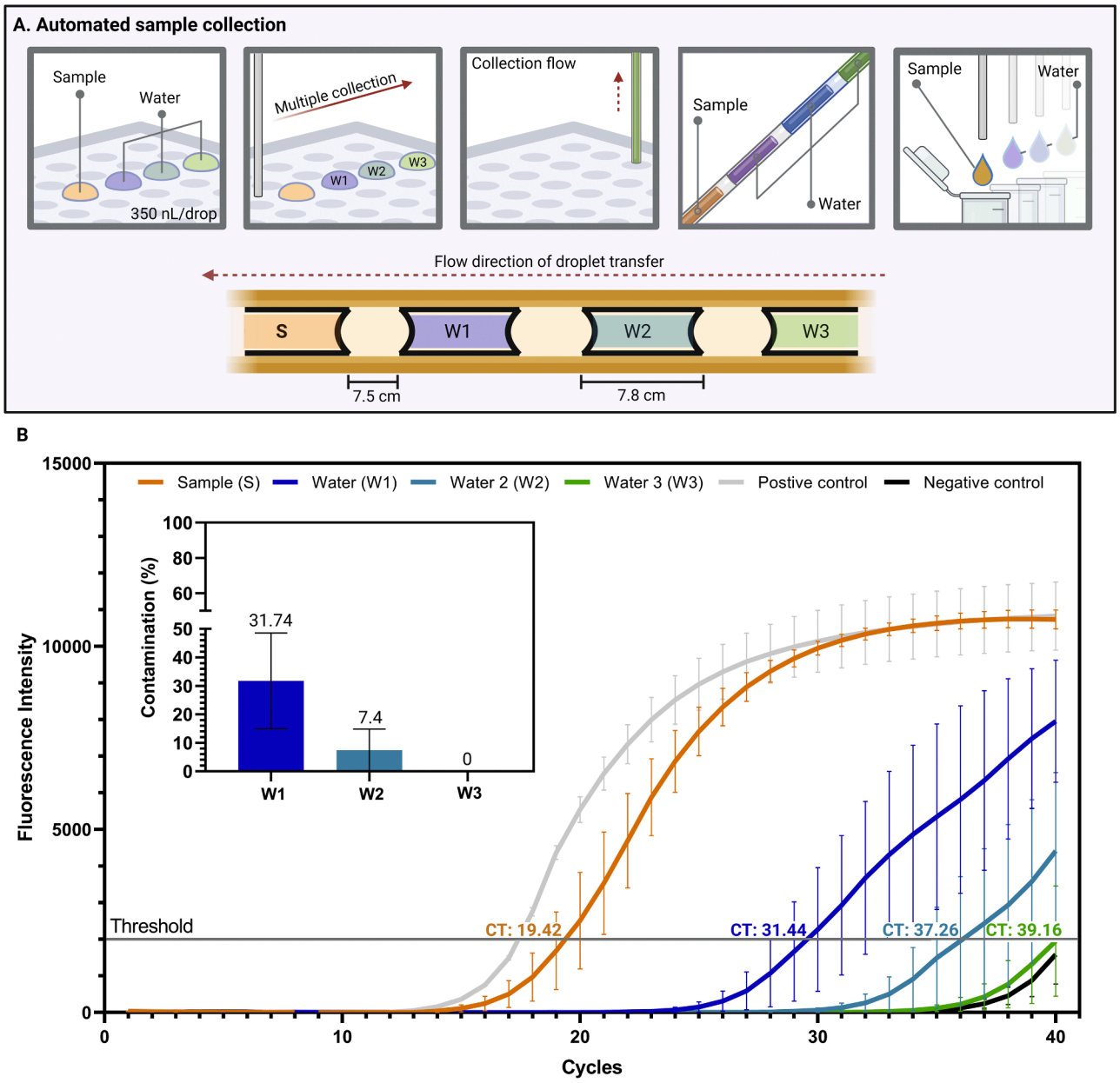

Fig. 7. Assessment of qPCR amplification of 350 nL droplets. (A) Schematic of the protocol for automated collection of nanoliter samples of cDNA and water from a DMA and subsequent droplet assignment in PCR tubes. For droplet collection, a fused silica capillary of 75 μm inner diameter and 80 cm length was used. The collection rate was set at 1 second per droplet, with an additional 1 second standby to create air gaps between the droplets. The first drop collected was the drop containing a concentration of 22.6 ng/μl of cDNA, followed by the 3 drops of water. After the collection process, the capillaries were removed from the ANDeS and closed at the ends with a silicon septum. The capillaries were then reinserted into the ANDeS syringe pump so that the cDNA sample was located at the opposite end to the one inserted into the pump. Subsequently, the samples were deposited in different PCR tubes using the syringe pump in infusion mode. Throughout this process, the capillaries were monitored with a microscope to observe the advancement of the droplets and ensure their accurate deposition into the PCR tubes which contained the qPCR master mix. Finally, the samples were evaluated for GAPDH gene expression via qPCR analysis. (B) qPCR amplification curves of individual cDNA and water droplets collected within the same capillary. The accompanying graph shows the percentage of contamination in the water samples. Error bars show the standard deviation between 3 replicates each.

equipment or for relocating droplets within a DMA slide. The ANDeS offers a positional accuracy of ±30 μm, allowing precise positioning of the capillary nozzle within a DMA slide down to 100 μm hydrophilic spots. This accuracy could be further improved if required. For example, in this version of ANDeS, each step taken by the stepper motor corresponds to a distance of 40 μm. However, by using leadscrews with a smaller pitch, such as 1.25 mm, the theoretical distance per step could be reduced to 6.25 μm, which would increase the accuracy of the system by a factor of six. Moreover, the incorporation of microstepping technology makes it possible to increase the accuracy even further. This technology allows the motor step size to be reduced from 1.8 °/step to 0.007 °/step, resulting in ≈ 50.000 steps per revolution instead [29].

ANDeS can also be adjusted to collect larger droplets. For this, the 100 μL syringe used for the first prototype of the machine, can be replaced with a syringe for larger volumes and the diameter and length of the capillaries can be increased. Alternatively, the syringe pump can be replaced by a continuous flow pump, facilitating a collection process unrestricted by the volume of the syringe. In addition, to increase the throughput of the system it is possible to modify the ANDeS Z-axis by adding a holder that accepts multiple capillaries at a time instead of just

one, which would provide faster bulk collection.

Using capillaries for multiple droplet collection has additional advantages in addition to efficient sample recovery from the DMA. These capillaries facilitate further processing of the collected samples, improving their handling, transport and storage while avoiding sample evaporation. For example, procedures such as ultrasound-mediated cell lysis and incubation of samples inside capillaries have been described [30,31]. In addition, the capillary format allows simultaneous injection of samples into the workflow of other analytical instruments. This feature is exemplified in the work of Chen et al. [32] where they introduced a configuration that allowed direct loading of protein samples from a capillary, attached to the injection pump, into a nanoLC-MS/MS system. Moreover, these methods can be further automated if the collection of these samples is performed automatically by robotics.

In the testing stage, we have successfully demonstrated the application of ANDeS for automated collection of samples for a real life experimental procedure. It enabled the analysis of cDNA samples contained in 350 nL droplets, eliminating the need for the previously reported manual pooling method described in [25]. This advancement resulted in a significant reduction of approximately 90 % in sample collection time while minimizing human error. In addition, manual collection restricts the optimal utilization of the DMA, as only a subset of available spots can be used in order to avoid sample merging when employing manual pooling. In contrast, automated droplet collection enables the utilization of all spots in the DMA without the risk of merging. It also eliminates the need of using chemical labels such as the Tandem Mass Tag (TMT) for subsequent sample identification after manual pooling, as was done in the study by Leduc et al. [33]. As a result, the use of ANDeS simplifies sample preparation, streamlines the protocol and reduces the need for exhaustive sample handling.

Overall, we have designed, fabricated and validated the ANDeS as a robotic system that extends the development of miniaturized assays within the DMA. ANDeS expands the compatibility of the DMA with various analytical equipment, including instruments such as LC-MS, NMR, and qPCR, as shown in this study. This broadening of possibilities increases the potential of DMA in droplet-based miniaturization research.

4. Conclusion

In this study, we developed an Automated Nanoliter Droplet Sorting and Collection (ANDeS) device, which addresses the challenges for collection and transfer of nanoliter droplets from the open Droplet Microarray (DMA) platform to another readout device or enables on-chip droplet-to-droplet manipulations. The system demonstrated its effectiveness in the collection of biological samples contained in nanodroplets for subsequent analysis, overcoming the limitations of manual collection techniques. In addition, ANDeS shows potential for scalability and high-throughput applications, enabling bulk sample collection and transfer to other analytical devices. By combining open-source robotics and off-the-shelf components, ANDeS offers a versatile and automated solution for miniaturized and parallelized assays.

5. Materials and methods

5.1. Design of the automated nanoliter droplet selection and collection device

The nano droplet manipulator is a Cartesian plane motion system composed of open source linear rails, carriages and transmissions (OpenBuilds Inc., New Jersey, USA), to which a syringe pump removed from a Micro Fraction Collector (Dionex Softron GmbH, Germering, Germany) was integrated to the system. This pump is equipped with a 100 μL 700 Series Syringe (Hamilton Inc., Reno, USA) coupled by applying reducing unions to a fused silica capillary (75 μm i.d., 360 μm o.d.; CS-Chromatographie Service GmbH, Langerwehe, Germany), which is fitted to the Z-axis using a 3D printer hot-end extruder (400 μm i.d; Shenzhen Redrex Technology Co., Ltd., Shenzhen, China) serving as a pipetting nozzle.

Nema 17 stepper (OpenBuilds Inc, New Jersey, USA) motors drive the 8 mm metric acme lead screws (OpenBuilds Inc, New Jersey, USA) of each axis and supply rotary power to the syringe pump assembly. These motors have a step angle of 1.8° per revolution, equivalent to 200 steps for one complete revolution [34] A4988 stepper motor drivers (Pololu Corporation, Nevada, USA) synchronize the rotation of each motor according to the pace and direction signals sent from the Raspberry Pi 4 model B (Raspberry Pi Foundation, Cambridge, England) through the Reprap Arduino Mega Pololu Shield 1.4 (ICQUANZX, Hong Kong, China).

The DMAs holder and adaptations were designed using Autodesk Fusion 360 (San Rafael, California) and produced on 3D printers by Creabis GmbH, Germany.

5.2. Motion characterization

To determine the motion characteristics of ANDeS, each axis was tested by moving from a given starting position, then moving a distance of 100 mm for the X and Y axes and 50 mm for the Z axis. The movement from the start point to the end point and vice versa was measured with a Mitutoyo 530–122 vernier caliper with a resolution of 0.02 mm (Mitutoyo, Kawasaki, Japan).

5.3. Droplet collection and transfer

The droplet microarray DMA slides were purchased from Aquarray GmbH, Eggenstein-Leopoldshafen, Germany. All the steps of automatic droplet printing were carried out using a universal liquid dispenser (I-DOT, Dispendix GmbH, Germany). The droplets were automatically collected and relocated by ANDeS through a fused silica capillary (75 μm i.d., 360 μm o.d.; CS-Chromatographie Service GmbH, Langerwehe, Germany). The drop height videos and pictures were taken with a x4 objective (Nikon x4 Plan Apo NA 0.20/20 mm) at 8-bit resolution. To measure the samples inside the capillaries, a Keyence BZ-9000 microscope (Keyence, Osaka, Japan) was used. The data analysis was carried out using ImageJ/Fiji (National Institutes of Health Inc, USA), GraphPad Prism (Dotmatics Inc, USA) and RStudio: Integrated development environment for R (Posit Inc, USA). The experimental times were taken with a digital stopwatch (A1000RCG-8B, Casio, Japan).

The images with color drops were made with drops of blue pen ink (Pelikan 4001, Pelikan Holding AG, Germany).

5.4. Sample transport and storage

The sample storage, preservation at 5 °C and transport were conducted by collecting the samples within the capillary, which was closed afterwards using silicone septum (3 mm, 9 mm Ø, CS-Chromatographie Service GmbH, Germany) as plugs to avoid evaporation or leaking.

5.5. mRNA extraction

The Cells-to-cDNA protocol was adapted and modified to accommodate suspension cells in this study. The original protocol, designed for adherent cells (Hela-CCL2), was adjusted to effectively synthesize cDNA from 400 SU-DHL-4 suspension cells printed per spot on the 672 spot DMA slide. The modifications incorporated into the protocol ensured the successful capture and processing of suspension cells, allowing for accurate cDNA synthesis and downstream analysis. The cells undergo lysis, followed by mRNA extraction and conversion into single-stranded cDNA for each spot. Subsequently, the collected samples are amplified using Terra PCR master mix (Takara Bio, Japan) to generate double-stranded cDNA. Quality control of the cDNA is performed, and the concentration

of the obtained cDNA is measured using the NanoDrop One microvolume UV–Vis spectrophotometers (Thermo fisher scientific Inc., USA) and checked for the cDNA quality via Agilent Bioanalyzer (Agilent technologies Inc., USA) . As a proof of concept, this experimental setup is designed to showcase the feasibility of the ANDeS. The previously synthesized cDNA is reprinted via a universal liquid dispenser (I-DOT, Dispendix GmbH, Germany) per spot with a total volume of 350 nL. Then cDNA is collected using ANDeS and subsequently quantified to assess the expression of a specific gene of interest via qPCR.

5.6. qPCR analysis

The cDNA droplets were collected from the capillary into a PCR microtube by using the ANDeS syringe pump. The capillary was attached to the microscope (Olympus CKX31, Japan) to monitor the movement of the droplets within the capillary ensuring that the droplets were collected completely in the previously chosen PCR tube. The qPCR was performed according to the manufacturer's protocol on a StepOne Real-time PCR system (Life Technologies GmbH, Germany).The GAPDH F & R primers (IDT) were utilized for this purpose. The Gotaq qPCR master mix (Promega GmbH, Germany), and the Biorad Thermal Cycler C1000 Touch™ (Thermo fisher scientific Inc., USA) was employed for the PCR amplification. The collected sample, with a total volume of 350 nL, is transferred into a qPCR tube along with the reagent mix to evaluate the expression of the GAPDH gene.

5.7. Statistical analysis

The measurement error for Fig. 4 and 5 was assessed by manually taking 10 measurements of a sample with predetermined drop height and length, respectively, using ImageJ/Fiji (National Institutes of Health Inc, USA). The confidence interval (95 %; 1.960 $\sigma_{\bar{x}}$) was calculated using the values of the mean and standard deviation of the experimental samples taken on each case. In Fig. 6 and 7 the mean and standard deviation were calculated from the raw data obtained from the StepOne Real-time PCR system (Life Technologies GmbH, Germany). The sample contamination percentages in Fig. 7 and the empirical model to describe *Flow* were calculated using RStudio: Integrated development environment for R (Posit Inc, USA). The calculations and plots were computed using GraphPad Prism (Dotmatics Inc, USA).

Creation of figures

The creation of the figures was done with Biorender.com.

Declaration of Competing Interest

The authors declare the following financial interests/personal relationships which may be considered as potential competing interests:

Joaquin E. Urrutia Gomez reports financial support was provided by German Academic Exchange Service. Anna A. Popova reports financial support was provided by Impuls und Vernetzungsfonds der Helmholtz-Gemeinschaft, Heidelberg and Karlsruhe cooperation program. Pavel A. Levkin reports financial support was provided by German Research Foundation. Pavel A. Levkin reports a relationship with Aquarray GmbH that includes: board membership. Anna A. Popova reports a relationship with Aquarray GmbH that includes: board membership.

Data availability

The data that support the findings of this study are available from the corresponding author upon reasonable request.

Acknowledgments

We gratefully acknowledge the funding sources that made this work possible: DFG (Heisenbergprofessur Projektnummer: 406232485, LE 2936/9–1), the Impuls und Vernetzungsfonds der Helmholtz-Gemeinschaft, Heidelberg and Karlsruhe cooperation program HEiKA, and the German Academic Exchange Service (DAAD).

Supplementary materials

Supplementary material associated with this article can be found, in the online version, at doi:10.1016/j.slast.2023.11.002.

References

[1] An WF, Tolliday N. Cell-based assays for high-throughput screening. Mol Biotechnol 2010;45(2):180–6.
[2] Gallert C, et al. High throughput screening system for screening of 3D cell cultures. In: Proceedings of the 2015 IEEE international instrumentation and measurement technology conference (I2MTC); 2015.
[3] Szymański P, Markowicz M, Mikiciuk-Olasik E. Adaptation of high-throughput screening in drug discovery—toxicological screening tests. Int J Mol Sci 2012;13:427–52. https://doi.org/10.3390/ijms13010427.
[4] Vyawahare S, Griffiths AD, Merten CA. Miniaturization and parallelization of biological and chemical assays in microfluidic devices. Chem Biol 2010;17(10):1052–65.
[5] Enders A, Grünberger A, Bahnemann J. Towards Small scale: overview and applications of microfluidics in biotechnology. Mol Biotechnol 2022:1–13.
[6] Feng W, et al. Surface patterning via thiol-yne click chemistry: an extremely fast and versatile approach to superhydrophilic-superhydrophobic micropatterns. Adv Mater Interfaces 2014;1(7):1400269.
[7] Feng W, Ueda E, Levkin PA. Droplet microarrays: from surface patterning to high-throughput applications. Adv Mater 2018;30(20):1706111.
[8] Lei W, et al. Droplet-microarray: miniaturized platform for high-throughput screening of antimicrobial compounds. Adv Biosyst 2020;4(10):2000073.
[9] Cui H, et al. Assembly of multi-spheroid cellular architectures by programmable droplet merging. Adv Mater 2021;33(4):2006434.
[10] Wiedmann JJ, et al. Nanoliter scale parallel liquid–liquid extraction for high-throughput purification on a droplet microarray. Small 2023;19(9):2204512.
[11] Popova AA, et al. Simple assessment of viability in 2D and 3D cell microarrays using single step digital imaging. SLAS Technol 2022;27(1):44–53.
[12] Tronser T, et al. Droplet microarray: miniaturized platform for rapid formation and high-throughput screening of embryoid bodies. Lab Chip 2018;18(15):2257–69.
[13] Benz M, et al. A combined high-throughput and high-content platform for unified on-chip synthesis, characterization and biological screening. Nat Commun 2020;11(1):5391.
[14] Benz M, et al. Marrying chemistry with biology by combining on-chip solution-based combinatorial synthesis and cellular screening. Nat Commun 2019;10(1):2879.
[15] Cui H, et al. Repurposing FDA-approved drugs for temozolomide-resistant IDH1 mutant glioma using high-throughput miniaturized screening on droplet microarray chip. Adv Healthc Mater 2023;12(24):e2300591.
[16] Seifermann M, et al. High-throughput synthesis and machine learning assisted design of photodegradable hydrogels. Small Methods 2023.;7(9):e2300553.
[17] Dong Z, Fang Q. Automated, flexible and versatile manipulation of nanoliter-to-picoliter droplets based on sequential operation droplet array technique. TrAC Trends Anal Chem 2020;124:115812.
[18] Zhu Y, et al. Sequential operation droplet array: an automated microfluidic platform for picoliter-scale liquid handling, analysis, and screening. Anal Chem 2013;85(14):6723–31.
[19] Du WB, et al. Automated microfluidic screening assay platform based on DropLab. Anal Chem 2010;82(23):9941–7.
[20] Li Q, et al. Automatic combination of microfluidic nanoliter-scale droplet array with high-speed capillary electrophoresis. Sci Rep 2016;6(1):26654.
[21] Jin DQ, Zhu Y, Fang Q. Swan probe: a nanoliter-scale and high-throughput sampling interface for coupling electrospray ionization mass spectrometry with microfluidic droplet array and multiwell plate. Anal Chem 2014;86(21):10796–803.
[22] Councill E, et al. Adapting a low-cost and open-source commercial pipetting robot for nanoliter liquid handling. SLAS Technol 2021;26(3):311–9.
[23] Zhu Y, et al. Nanodroplet processing platform for deep and quantitative proteome profiling of 10–100 mammalian cells. Nat Commun 2018;9(1):882.
[24] Florian DC, et al. Principles of computer-controlled linear motion applied to an open-source affordable liquid handler for automated micropipetting. Sci Rep 2020;10(1):13663.
[25] Chakraborty S, et al. Cells-to-cDNA on chip": phenotypic assessment and gene expression analysis from live cells in nanoliter volumes using droplet microarrays. Adv Healthc Mater 2022;11(12):2102493.
[26] Caraguel CG, et al. Selection of a cutoff value for real-time polymerase chain reaction results to fit a diagnostic purpose: analytical and epidemiologic approaches. J Vet Diagn Invest 2011;23(1):2–15.

[27] Meyer JN. QPCR: a tool for analysis of mitochondrial and nuclear DNA damage in ecotoxicology. Ecotoxicology 2010;19(4):804–11.
[28] Tian Y, et al. Development of a reverse-transcription droplet digital PCR method for quantitative detection of cucumber green mottle mosaic virus. Heliyon 2023;9 (2):e12643.
[29] Matsuo K, et al. Maximum torque micro-step drive of a five-phase hybrid stepping motor. IEEJ Trans Electr Electron Eng 2023;18(3):491–3.
[30] Shao X, et al. Integrated proteome analysis device for fast single-cell protein profiling. Anal Chem 2018;90(23):14003–10.
[31] Matzinger M, Mayer RL, Mechtler K. Label-free single cell proteomics utilizing ultrafast LC and MS instrumentation: a valuable complementary technique to multiplexing. Proteomics 2023;23(13–14):e2200162.
[32] Chen Q, et al. Ultrasensitive proteome profiling for 100 living cells by direct cell injection, online digestion and nano-LC-MS/MS analysis. Anal Chem 2015;87(13): 6674–80.
[33] Leduc A, et al. Exploring functional protein covariation across single cells using nPOP. Genome Biol 2022;23(1):261.
[34] Deshmukh SP, Shewale MS, Suryawanshi V, Manwani A, Singh VK, Vhora R, et al. Design and development of xyz scanner for 3d printing. In: *2017 International Conference on Nascent Technologies in Engineering (ICNTE)*. IEEE; 2017. p. 1–5.